CARBON 92 (2015) 297–304

Available at www.sciencedirect.com

ScienceDirect

journal homepage: www.elsevier.com/locate/carbon

Highly selective CO_2 capture by nitrogen enriched porous carbons

Hailin Cong [b,1], Meirong Zhang [a,b,1], Yanli Chen [a], Kai Chen [a], Yajuan Hao [a], Yunfeng Zhao [a,*], Lai Feng [a,*]

[a] College of Physics, Optoelectronics and Energy & Collaborative Innovation Center of Suzhou Nano Science and Technology, Soochow University, Suzhou 215006, China

[b] Lab for New Fiber Materials and Modern Textile-Growing Base for State Key Laboratory, College of Chemical and Environmental Engineering, Qingdao University, Qingdao 266071, China

ARTICLE INFO

Article history:
Received 11 February 2015
Accepted 20 April 2015
Available online 25 April 2015

ABSTRACT

A series of nitrogen enriched microporous carbons were facilely prepared by KOH activation using melamine-doped phenolic resins as precursors. The activated carbons show high CO_2 uptakes up to ca. 1.3 mmol g^{-1} under low pressure (0.15 bar, 25 °C), which can be ascribed to not only their optimal fraction of ultramicropores but also the high N-contents. One of the samples even exhibits excellent adsorption selectivity for CO_2 over N_2 (*i.e.*, selectivity factors of 43.7 and 52.9 obtained from initial slope and IAST calculations, respectively). Furthermore, the preferential CO_2 uptake of the carbons was confirmed by successive breakthrough experiments under post combustion flue gas stream conditions (15% CO_2 concentration, 1 bar and 25 °C). Since these carbons also feature good stability over repeated thermal cycling and ease of regeneration, their practical applications in post combustion CO_2 capture shall lie within the realm of possibility.

1. Introduction

In the past decades, global warming has been emerging as an international issue, which was attributed to the increasing emissions of greenhouse gas such as CO_2, CH_4 and so on [1]. Particularly, it has been generally believed that the energy-related CO_2 emissions contribute to the major component of greenhouse gas. To date, extensive efforts have been devoted to developing CO_2 capture and storage technologies [2–4], aiming to substantially reduce CO_2 emissions under the premise of ensuring the normal operation of power-plant. Over the last few years, the technologies of post-combustion CO_2 capture have been rapidly developed [5]. Various adsorbents were prepared and employed for this purpose [6]. Nevertheless, given the low content (*i.e.*, ~15%) or low partial pressure of CO_2 in the flue gas streams [7,8], real application requires developing the adsorbents with high CO_2 adsorption capacity at low pressure and high selectivity of CO_2 over other gases such as N_2, the major component of the flue gas.

In recent years, a variety of porous solid sorbents such as metal-organic frameworks (MOFs) [9,10], covalent organic frameworks (COFs) [11–13], zeolites [14,15], metal oxides [16,17] and porous carbons [18–24] have been developed for CO_2 capture. Among them, MOF materials exhibited the highest CO_2 uptake up to 8.5 mmol g^{-1} at ambient conditions (*i.e.*, 25 °C and 1 bar) [25]. Nevertheless, most of MOF materials

* *Corresponding authors.*
E-mail address: fenglai@suda.edu.cn (L. Feng).
[1] Hailin Cong and Meirong Zhang contributed equally to this work.
http://dx.doi.org/10.1016/j.carbon.2015.04.052
0008-6223/

feature high-cost and low stability toward ambient moisture, which make them not suitable for practical use. In contrast, microporous carbons show several advantages such as superior thermal/chemical stabilities, low cost, tunable pore structures and easy regeneration as well, indicating their superior potential for post-combustion CO_2 capture.

To improve the application of microporous carbons, continuous interests focus on the development of simple preparation routes to the carbons with high CO_2 capture capacities. As suggested by literatures, one particular simple methodology is to activate the less porous carbons chemically or physically, resulting in highly microporous carbons that deliver high CO_2 uptake in the range of 3–5 mmol g^{-1} at ambient conditions (*i.e.*, 25 °C and 1 bar) [26–31]. For instance, carbonaceous phenolic resins showed limited CO_2 uptake, whereas the CO_2 or KOH activated carbons exhibited remarkably improved CO_2 adsorption capacities [21,27].

On the other hand, some literatures also reported that microporous carbons with doped heteroatoms displayed enhanced CO_2 uptake especially at low pressure as well as high CO_2/N_2 selectivity, though the contributions of the doped heteroatoms (*i.e.*, N, S) are still under controversial [32–36]. To date, the best performing N-doped carbons exhibited CO_2 uptake reaching 1.51 mmol g^{-1} (at 0.15 bar and 25 °C) and good CO_2/N_2 selectivity as well [34], indicative of their potential application for CO_2 and N_2 separation.

In this work, we report on a family of N-enriched microporous carbons prepared via one-step KOH activation of melamine-doped phenolic resins. Particularly, by adjusting the activation conditions as well as the melamine contents in the phenolic precursors, it is possible to obtain the carbons displaying high CO_2 uptake of ca. 1.3 mmol g^{-1} at 0.15 bar, 25 °C and high CO_2/N_2 selectivity up to 52.9 and 43.7 (calculated by IAST or initial slope method, respectively). The study also provides further experimental evidence on the importance of not only the ultramicropores but also the N-species for preferential CO_2 uptake at low pressure. Moreover, to evaluate the potential of utilizing these N-enriched microporous carbons for post combustion CO_2 capture, their CO_2 uptake capacity under kinetic flue gas condition and the regeneration capability are properly assessed.

2. Experimental

2.1. Preparation of N-enriched microporous carbons

The melamine-doped phenolic-resins were prepared using a recipe reported by Zhou et al. [37]. Briefly, 1.125 g of resorcinol and 1.658 g of formaldehyde water solution (37 wt%) were dissolved in 19.5 mL of distilled water and then stirred for more than 1 h. Meanwhile, 1.288 g of melamine and 2.488 g of formaldehyde water solution were dissolved in 60 mL of distilled water at 80 °C. The solution was stirred vigorously until the solution became clear and slowly cooling down to 40 °C. Subsequently, the two solutions were mixed and stirred for 30 min. in which the molar ratio of melamine to resorcinol is 1:1. Then, the mixed solution was transferred in a Teflon-lined steel autoclave and treated at 120 °C for 24 h. After polymerization, the obtained yellowish resins (MR-1) were freeze-dried in vacuum overnight. By increasing the ratio of melamine and resorcinol to 1.5 and 3, respectively, we also prepared the resins MR-1.5 and MR-3.

The post-synthesis activations of these MR resins were performed by placing a molybdenum boat with a mixture of 1 g as-prepared MR resins and 0.25 g KOH in a tube furnace under flowing nitrogen with a heating rate of 3 °C min^{-1} up to 500–700 °C. The mixture was kept at the target temperature for 40 min and the resulting samples were washed with 1 M HCl, then deionized water to remove potassium salts, and dried. The obtained carbonaceous materials were labeled as MR-*x*-*y*, where *x* refers to the ratio of melamine to resorcinol (*i.e.*, 1, 1.5 or 3) and *y* refers to the activation temperature in °C (*i.e.*, 500, 600 or 700).

2.2. Characterization

Scanning electron microscopy (SEM) images were obtained with a Hitachi SU8010 instrument. Transmission electron microscopy (TEM) was conducted on a FEI TecnaiG220 instrument at 200 kV accelerating voltage. The Fourier transform infrared (FT-IR) spectra were obtained on a TENSOR27 spectrometer (Bruker, Germany) with sample prepared as KBr pellets. X-ray photoelectron spectroscopy (XPS) studies were carried out with an ESCALAB 250 spectrometer using a monochromated Al Kα excitation source. Nitrogen adsorption–desorption isotherms at −196 °C and CO_2 adsorption isotherms at 0 and 25 °C were all measured on an adsorption volumetric analyzer ASAP 2020 manufactured by Micromeritics, Inc. (Norcross, Georgia, USA). All samples were degassed at 200 °C overnight prior to adsorption measurements. A part of the N_2 sorption isotherm in the p/p_0 range of 0.005–0.05 was fitted to the BET equation to estimate the BET surface area (see Fig. S1) [38,39]. Total pore volume (PV_t) was obtained at a relative pressure of 0.985. The pore size distribution (PSD) was obtained from the DFT model in the Micromeritics ASAP 2020 software package (assuming slit pore geometry) based on the CO_2 adsorption at 0 °C. The micropore surface areas were determined using the nonlocal density theory (NLDFT) method.

The breakthrough separation experiments were conducted on a homemade apparatus as previously described [32]. In a typical experiment, 550 mg of porous carbon sorbent (MR-1.5-500) was thoroughly grounded and packed into a quartz column (5.8 mm I.D. × 150 mm) with silica wool filling the void space. The sorbent in the column was activated with a helium flow (10 mL min^{-1}) at 200 °C for 1 h and then the column was cooled down to 25 °C. The flow of He was then turned off while a gas mixture of N_2/CO_2 (85:15, v/v) at 5.0 mL min^{-1} was sent into the column. The effluent from the column was monitored using a mass spectrometer (Pfeiffer vacuum; OmniStar, GSD 320). Other details for calculating the adsorption capacity and CO_2/N_2 selectivity are also previously described [32]. The CO_2 saturated sample was regenerated in situ by purging the column with a helium flow (10 mL min^{-1}) at 80 °C for 0.5 h and then cooled down to 25 °C for the next breakthrough cycle.

3. Results and discussion

3.1. Structural properties of the activated carbons

In the previous studies, a variety of phenolic resins were synthesized and further subject to activations for preparing microporous carbons [21,40–42]. Nevertheless, previously reported carbons derived from N-enriched phenolic resins showed lower CO_2 uptakes than expected [35,40–42], though it has been proposed that the presence of nitrogen groups on the carbon surface can promote CO_2 capture capacity. Herein, we use melamine-doped phenolic-resins as precursors for preparing N-enriched microporous carbons. After polymerization, the resulting MR-x (x = 1, 1.5, 3) resins were directly subjected to KOH activations under nitrogen without having to be pre-carbonized. Noteworthy is that in this study the carbonization and activation were carried out in a combined (one step) procedure, while the two processes were usually separated in most of reported porous carbon preparations due to the instability of as-prepared polymers under highly basic condition [32,33]. Thus, this one-step method would render these porous carbons the advantage of simple preparation, which makes them competitive adsorbents for practical application in flue gas treatment.

The morphologies of the activated carbons were studied with scanning electron microscopy (SEM). As can be seen in Figs. 1a and S2, the as-prepared MR precursors show particle morphology, while the activated carbons feature mainly large monoliths, suggesting the significant morphological change of the polymeric carbons during the activation process. To further understand the micro-structures of the activated carbons, transmission electron microscopy (TEM) measurements were carried out. As shown in Figs. 1c and S3, the disordered slit-like micropores can be clearly seen in the typically activated samples MR-x-500, suggesting their microporous structures.

On the other hand, elemental mappings by means of SEM (Fig. 1b) demonstrated that the doped nitrogen species are uniformly distributed in the activated carbons. The nature of the doped nitrogen species was further investigated by means of X-ray photoelectron spectroscopy (XPS). As shown in Figs. 2 and S4, the carbons obtained under different activation conditions exhibit similar XPS spectra, in which the N1s signal can be fitted by three peaks with binding energies centered at 398.4 eV, 400.0 eV and 401.3 eV, representing pyridinic N, pyrrolic N and graphitic N, respectively. It is noteworthy that among these N-contents the pyrrolic N is generally more abundant than others, which is beneficial for the CO_2 capture [23]. Moreover, as determined by XPS, the N-contents of MR-1-y series are in the range of 3.8–4.9%, while MR-1.5-y and MR-3-y contain higher N-contents up to 6.4–8.2% (see Table S1). Thus, it is apparent that increasing the melamine contents in precursors resulted in, as expected, N-enriched carbons. In addition, the presence of N-species in the activated carbons was also verified with FT-IR spectroscopy. Specifically, Fig. S5a shows the characteristic stretching modes of the N-H and C-N functionalities at 3428–3410 and 1212–1092 cm^{-1}, respectively, confirming the presence of these N-species in the activated carbons. In other region, Fig. S5a also displays

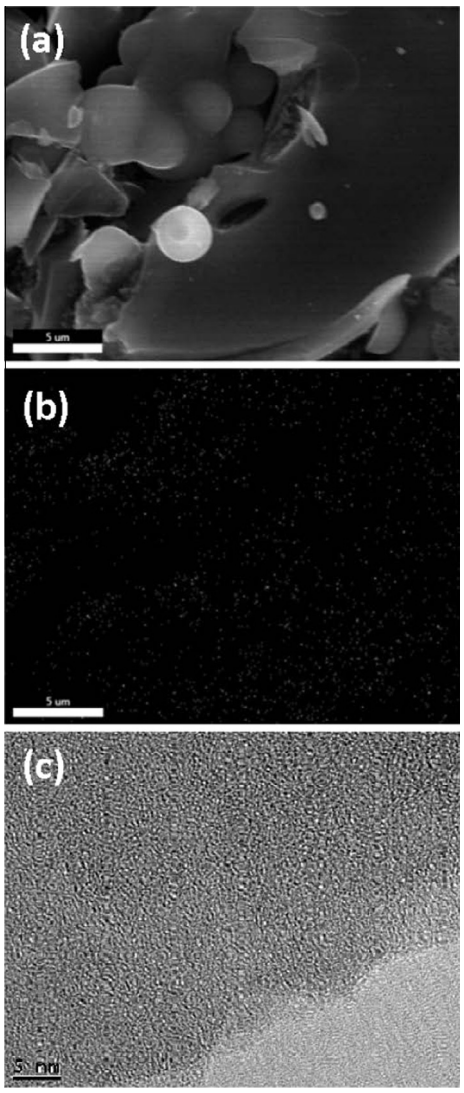

Fig. 1 – (a) SEM image, (b) nitrogen mapping and (c) TEM image of the sample MR-1-500.

typical C=N stretching modes at ca. 1557 and 1490 cm^{-1}, which are much weaker relative to those seen in the FT-IR spectra of the as-prepared MR-x precursors (see Fig. S5b), indicating the significant reduction of C=N functionality during the activation process.

3.2. BET surface area

To investigate the porous characteristics of these activated carbons, nitrogen adsorption–desorption measurements were carried out at −196 °C. All measured isotherms are presented in Fig. 3, while the specific surface area and pore structure parameters are listed in Table 1. As can be seen from Fig. 3 and Table 1, these activated carbons are highly porous. Among all these samples, MR-3-600 possesses the highest surface area of 1620 $m^2 g^{-1}$ as well as the largest total pore volume of 0.836 $cm^3 g^{-1}$. In general, the BET surface areas of these microporous carbons increase with increasing the activation temperature in a range of 500–700 °C. Noteworthy is that most isotherms feature a typical adsorption plateau at

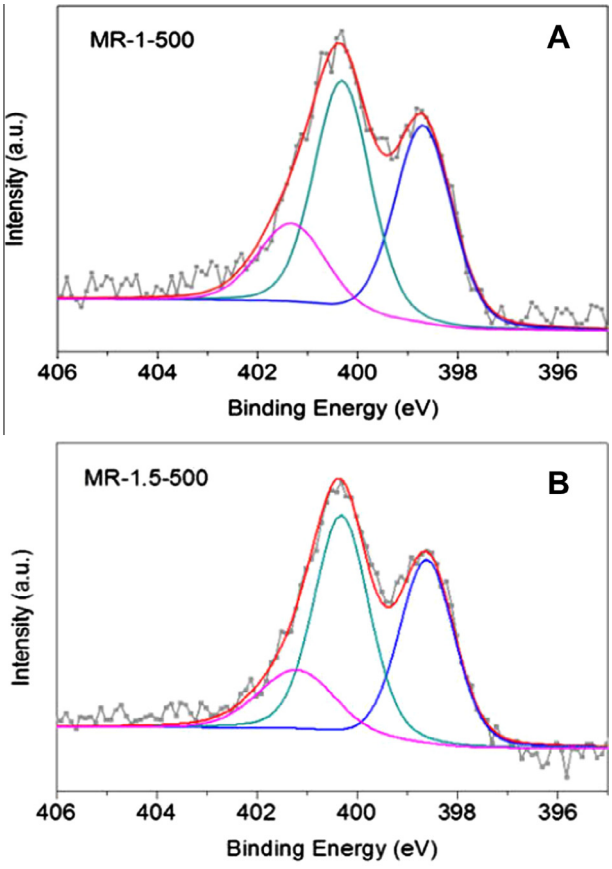

Fig. 2 – N1s XPS spectra of the samples MR-1-500 (A) and MR-1.5-500 (B). (A color version of this figure can be viewed online.)

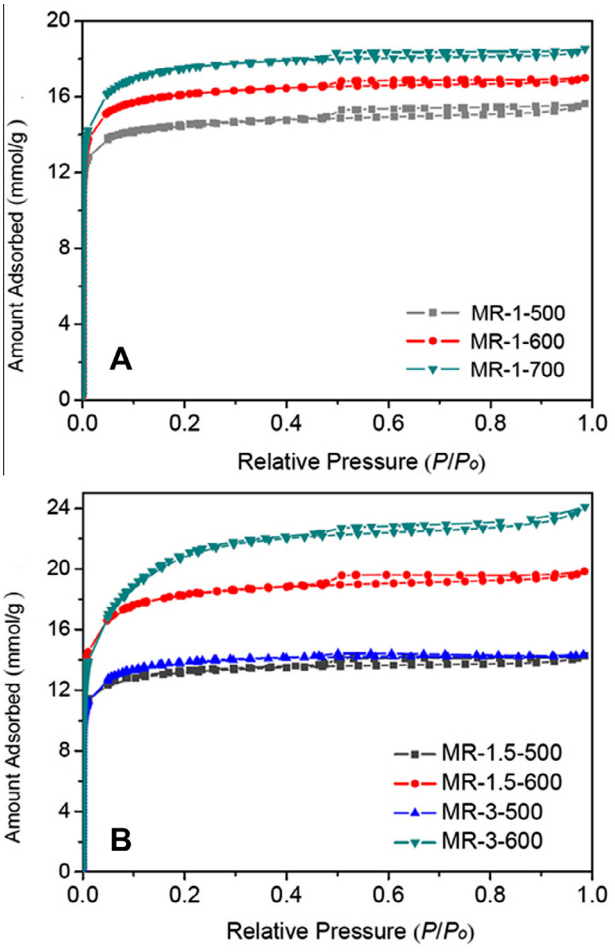

Fig. 3 – Nitrogen adsorption isotherms for MR-1-y series (A), MR-1.5-y and MR-3-y series (B). (A color version of this figure can be viewed online.)

low relative pressure and can be assigned to type I, indicating the presence of large fraction of micropores in these activated carbons. Moreover, all isotherms also display small hysteresis loops at moderate to high relative pressure, suggesting the presence of a small fraction of mesopores for all these samples. Cumulative pore volume curves obtained from low temperature N_2 adsorption using density functional theory (DFT) method for slit-type pore geometry are presented in Fig. S6. These data suggest that for most activated carbons (except for MR-3-600) their cumulative pore volumes are mainly derived from the pores smaller than 1.5 nm, indicating a large potential for CO_2 adsorption.

3.3. *CO_2 adsorption capacity*

The CO_2 adsorption capacities of these N-doped activated carbons were investigated at 0 and 25 °C under atmospheric pressure (1 bar). All the measured CO_2 adsorption isotherms are presented in Figs. 4, S7, and the related data are listed in Table 1. It is interesting to note that the sample MR-1-500 shows higher CO_2 uptake at 1 bar (25 or 0 °C) or low pressure (0.15 bar, 25 °C) with respect to other samples, despite of its moderate BET surface area of 1286 $m^2 g^{-1}$. To the best of our knowledge, the CO_2 uptake of 1.31 mmol g^{-1} at low pressure (0.15 bar) and 25 °C is even comparable to the highest ever reported for various phenolic-resin-derived carbons [20,26]. Moreover, the uptakes of MR-1.5-500 and MR-3-500 are determined to be 1.29 mmol g^{-1} at low pressure (0.15 bar) and 25 °C, though their surface areas are much lower than those of other samples. These results clearly show that the CO_2 adsorption capacities of the activated carbons are not closely related to their surface areas.

To further investigate how the structural properties of micropores influence the CO_2 adsorption capacities of these activated carbons, the cumulative pore volume curves derived from fine micropores with size smaller than 1.1 nm as well as their pore size distributions were calculated using DFT method and assuming slit-type pore geometry (see Figs. S8 and S9). The resulting data (Table S1 and Fig. S10) likely suggest that the micropores with size below 0.7 nm are more important than the larger micropores in determining the CO_2 uptakes of these activated carbons under ambient conditions (*i.e.*, 1 bar and 25 °C). Typically, among the MR-x-500 series, MR-1-500 has the highest ultramicropore volume (*i.e.*, $PV_{0.7nm}$), followed by MR-1.5-500 and MR-3-500. The CO_2 uptake of MR-1-500 (*i.e.*, 4.04 mmol g^{-1} at 1 bar and 25 °C) is consistently higher than those of MR-1.5-500 and MR-3-500 (*i.e.*, 3.77 and 3.51 mmol g^{-1} at 1 bar and 25 °C) by 7% and 15%, respectively. These results agree well with the previous reports, which demonstrated a good correlation between the

Table 1 – Physical characteristics of N-doped microporous carbons.

Sample	N_2 adsorption at −196 °C			CO_2 adsorption at 0 °C		CO_2 uptake (mmol g^{-1})		
	S_{BET} (m^2 g^{-1})	PV_t (cm^3 g^{-1})	$PV_{1.5nm}$ (cm^3 g^{-1})	S_{nm} (m^2 g^{-1})	$PV_{0.7nm}$ (cm^3 g^{-1})	25 °C 1 bar	25 °C 0.15 bar	0 °C 1 bar
MR-1-500	1286	0.542	0.442	1097	0.132	4.04	1.31	6.24
MR-1-600	1428	0.589	0.451	1094	0.113	3.92	1.22	6.05
MR-1-700	1531	0.643	0.531	1058	0.083	3.44	0.98	5.67
MR-1.5-500	1159	0.494	0.382	1026	0.110	3.77	1.29	5.80
MR-1.5-600	1579	0.688	0.539	1093	0.086	3.56	0.99	5.88
MR-3-500	1196	0.498	0.394	996	0.094	3.51	1.29	5.28
MR-3-600	1620	0.836	0.473	1176	0.080	3.36	0.89	5.99

S_{BET}: specific surface area calculated by the Brunauer–Emmett–Teller (BET) method (p/p_0 = 0.005–0.05). PV_t: total pore volume at p/p_0 = 0.985. $PV_{1.5nm}$: cumulative pore volume calculated in the range of pore widths up to 1.5 nm; S_{nm} and $PV_{0.7nm}$: the surface area and volume of narrow micropores (<0.7 nm) calculated with the DFT model, respectively.

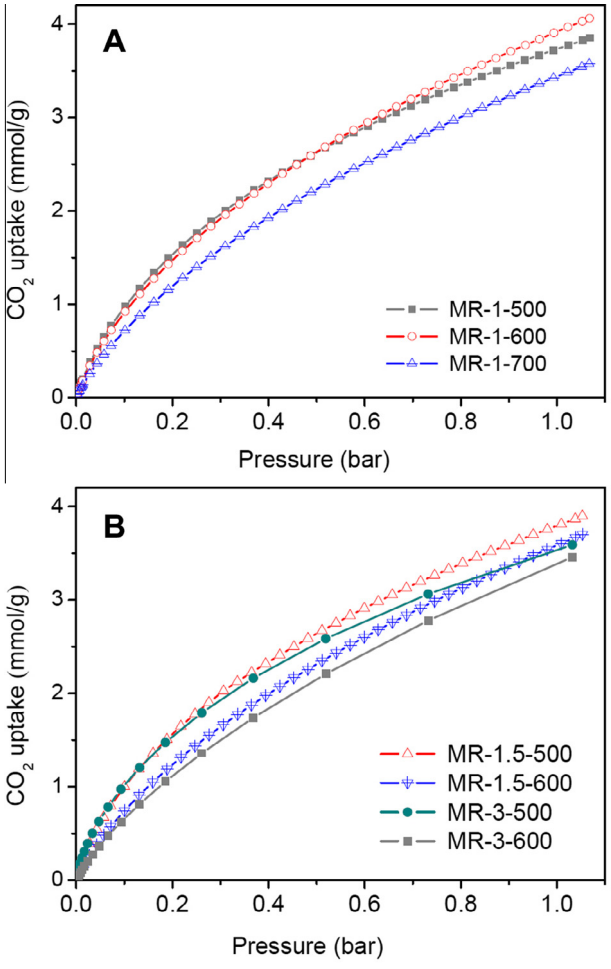

Fig. 4 – CO_2 adsorption isotherms for MR-1-y series (A), MR-1.5-y and MR-3-y series (B) measured at 25 °C. (A color version of this figure can be viewed online.)

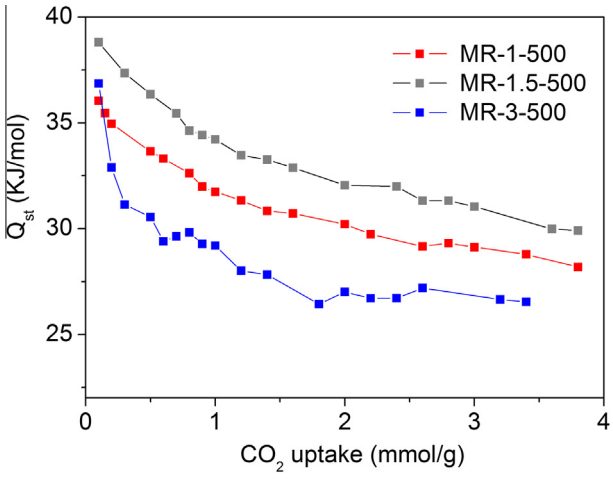

Fig. 5 – Isosteric heat of CO_2 adsorption on MR-1-500, MR-1.5-500 and MR-3-500 calculated from the experimental adsorption isotherms obtained at 0 and 25 °C. (A color version of this figure can be viewed online.)

volume of the micropores smaller than 1 or 0.8 nm and the CO_2 uptake under ambient conditions [29,43]. However, MR-x-500 series showed similar CO_2 uptakes at low pressure (*i.e.*, 0.15 bar) and 25 °C (*i.e.*, 1.29–1.31 mmol g^{-1}), though their ultramicropore volumes are quite different. We ascribe these similar uptakes to the fact that the samples MR-1.5-500 and MR-3-500, despite having lower ultramicropore volumes, possess much higher N-contents, while the sample MR-1-500 has lower N-content but higher ultramicropore volume. This observation demonstrates the importance of N-content in determining the low pressure CO_2 uptake at 25 °C. Therefore, it is rational to propose a combined influence of ultramicropores and N-species on low pressure (0.15 bar) CO_2 uptake, while at ambient pressure (1 bar), ultramicropores play a more crucial role.

In addition, based on the data discussed above, the optimized activation temperature is determined as 500 °C. The samples activated at this temperature possess higher ultramicropore volume and, thus, show higher CO_2 uptakes relative to others. Increasing the activation temperature causes reduced ultramicropore volume and lower CO_2 uptake. On the other hand, varying the M/R ratio in precursor gave rise to more complex results. Particularly, increasing the M/R ratio from 1 to 1.5 and 3 results in the carbons having higher N-content, larger BET surface area but lower ultramicropore volume (see Table 1). It is thus possible to vary the structural

Table 2 – CO_2/N_2 selectivity factors calculated using initial slope method (IS) and IAST model, respectively.

Sample	MR-1-500	MR-1-600	MR-1-700	MR-1.5-500	MR-1.5-600	MR-3-500	MR-3-600
IS	27.5	30.5	23.4	43.7	24.7	37.2	17
IAST	28.4	31.2	22.6	52.9	23.0	48.7	21.5

properties and CO_2 uptake capacities of the activated carbons by simply choice of the activation temperature and the M/R ratio in precursor.

To better understand the CO_2 adsorption capacities of these N-doped activated carbons, their isosteric heats of adsorption (Q_{st}) were calculated using adsorption isotherms obtained at 0 and 25 °C, respectively. As shown in Fig. 5, the calculated Q_{st} values of MR-x-500 series are in the ranges of 36.1–28.2 ($x = 1$), 38.8–29.9 ($x = 1.5$) and 36.9–26.5 ($x = 3$) kJ mol^{-1}, respectively. These values are much higher than those obtained from the non-doped microporous carbons with comparable CO_2 uptakes at low pressure (*i.e.*, 27.7–20.3 kJ mol^{-1}) [26], suggesting the strong interaction between CO_2 and the surface of these N-doped microporous carbons.

3.4. *Selectivity for CO_2 adsorption*

As typical flue gas stream contains only ~15% CO_2 with the rest being mainly N_2 and a small amount of water vapor [6], the post-combustion CO_2 capture technology requires the sorbents with high CO_2/N_2 selectivity. To estimate the CO_2/N_2 selectivities for these N-enriched microporous carbons, the N_2 adsorption isotherms at 0 and 25 °C were also measured for comparison with the CO_2 isotherms. As shown in Fig. S12, the samples MR-x-500 ($x = 1, 1.5, 3$) show very limited N_2 uptakes which are much lower than their CO_2 uptakes at the same temperature, indicative of high CO_2/N_2 selectivities. Furthermore, initial slope calculations based on CO_2 and N_2 adsorption isotherms [44] were performed to determine the CO_2/N_2 selectivities of the carbons (see Table 2). Particularly, MR-x-500 ($x = 1, 1.5, 3$) series give the selectivity factors of 27.5, 43.7 and 37.2, respectively. The factor of 43.7 is even comparable to the highest CO_2/N_2 selectivity ever reported (*i.e.*, a selectivity factor of 43 calculated using the same method) [31].

The ideal adsorbed solution theory (IAST) model [45,46] was also used to estimate the selectivity of CO_2 over N_2 for all the samples. The calculated results are shown in Figs. 6, S14 and listed in Table 2, which are all consistent with the factors obtained using initial slope method. Specifically, superior IAST selectivity factors of 28.4, 52.9 and 48.7 were obtained for MR-1-500, MR-1.5-500 and MR-3-500, respectively, at the total pressure of 1 bar and 15% CO_2 concentration. The IAST selectivity of MR-1.5-500 is also among the highest reported for known carbon materials under similar condition [31,32], indicating an excellent CO_2 capture capacity from a flue gas stream. According to the results discussed above, we propose that very high CO_2/N_2 selectivity of MR-1.5-500 is due to not only its optimal $PV_{0.7nm}$ but also the high N-content.

Moreover, to evaluate the potential of these carbons for post-combustion applications, breakthrough experiments were carried out to estimate the CO_2 capture capacity from a CO_2/N_2 mixture (15:85, v/v) under kinetic flow conditions. As shown in Fig. 7, when the flue gas passed through a sorbents-filled column, N_2 was detected at an earlier stage, while CO_2 was detected with a delayed time of 463 s. The CO_2 adsorption capacity and CO_2/N_2 selectivity for MR-1.5-500 were calculated to be 2.1 wt% and 45, respectively, consistent with the IS or IAST selectivity derived from the single gas adsorption isotherms. To test the regeneration capability of

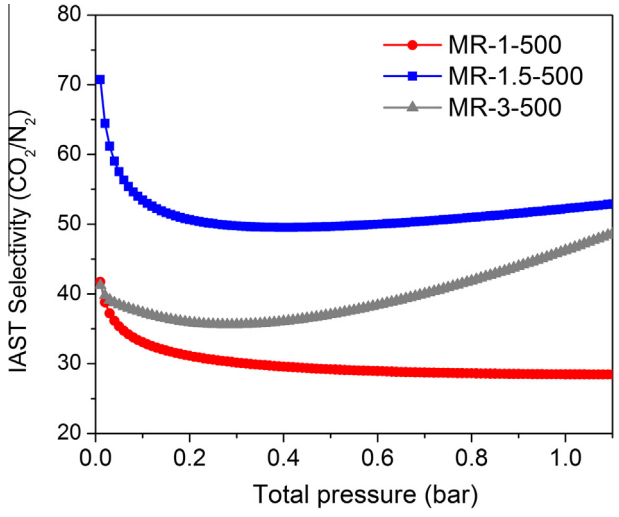

Fig. 6 – The IAST-predicted selectivity for MR-x-500 series with the overall pressure of 1 bar at 25 °C. (A color version of this figure can be viewed online.)

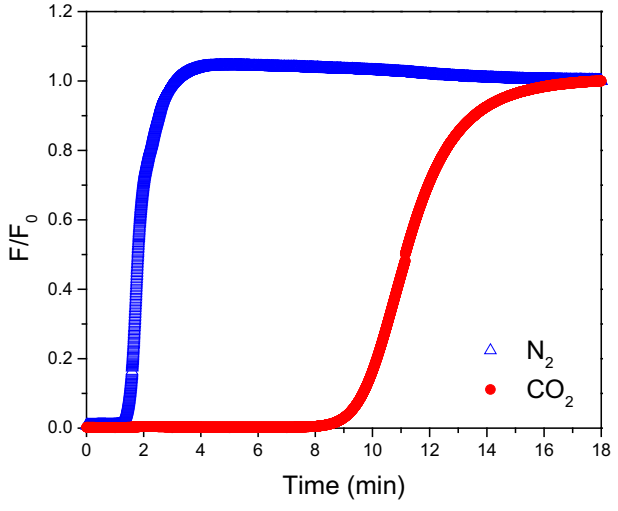

Fig. 7 – Column breakthrough curves for a CO_2–N_2 (15:85, v/v) in 5 mL min^{-1} mixed gas at 25 °C and 1 bar over MR-1.5-500. (A color version of this figure can be viewed online.)

these carbons, we also performed successive breakthrough experiments on the representative sample of MR-1.5-500, which showed almost constant CO_2 adsorption capacities and good CO_2/N_2 selectivities over ten cycles (see Fig. S15), indicating that these materials can be repeatedly regenerated under mild conditions.

4. Conclusions

In summary, we have prepared a series of nitrogen enriched microporous carbons by one-step KOH activation under mild conditions using melamine-doped phenolic resins as precursors. Three of the prepared samples (*i.e.*, MR-*x*-500) show high CO_2 uptakes of ca. 1.3 mmol g^{-1} under low pressure (0.15 bar and 25 °C), which can be ascribed to not only their optimal fraction of ultramicropores but also the high N-contents. One of the samples (*i.e.*, MR-1.5-500) even shows excellent adsorption selectivity for CO_2 over N_2 (*i.e.*, selectivity factors of 43.7 and 52.9 given by the initial slope and IAST calculations, respectively). Furthermore, this preferential CO_2 capture was confirmed by a breakthrough experiment under post combustion flue gas stream conditions. The successive experiments additionally suggest that the carbons can be facilely regenerated and show good stability over several adsorption–desorption cycles. Thus, considering the combined characteristics of these carbons, including simple preparation, high CO_2 uptake at low pressure, excellent CO_2/N_2 selectivity, ease of regeneration and nice cyclability, they might be suitable sorbents for post-combustion CO_2 capture.

Acknowledgements

This work is the supported in part by the NSFC (51372158), NTP (20133201120004), Jiangsu Specially Appointed Professor Program (SR10800113), the Project for Jiangsu Scientific and Technological Innovation Team (2013).

Appendix A. Supplementary data

Supplementary data associated with this article can be found, in the online version, at http://dx.doi.org/10.1016/j.carbon.2015.04.052.

REFERENCES

[1] Haszeldine RS. Carbon capture and storage: how green can black be? Science 2009;325(5948):1647–52.
[2] Smol JP. Climate change: a planet in flux. Nature 2012;483(7387):s12–5.
[3] Yang H, Xu Z, Fan M, Gupta R, Slimane RB, Bland AE, et al. Progress in carbon dioxide separation and capture: a review. J Environ Sci 2008;20(1):14–27.
[4] Yong Z, Mata V, Rodrigues AE. Adsorption of carbon dioxide at high temperature – a review. Sep Purif Technol 2002;26(2–3):195–205.
[5] Samanta A, Zhao A, Shimizu GKH, Sarkar P, Gupta R. Post combustion CO_2 capture using solid sorbents: a review. Ind Eng Chem Res 2011;51(4):1438–63.
[6] Kim J, Lin L-C, Swisher JA, Haranczyk M, Smit B. Predicting large CO_2 adsorption in aluminosilicate zeolites for post combustion carbon dioxide capture. J Am Chem Soc 2012;134(46):18940–3.
[7] Figueroa JD, Fout T, Plasynski S, McIlvried H, Srivastava RD. Advances in CO_2 capture technology—The U.S. department of energy's carbon sequestration program. Int J Greenhouse Gas Control 2008;2(1):9–20.
[8] Zhang Z, Wang K, Atkinson JD, Yan X, Li X, Rood MJ, et al. Sustainable and hierarchical porous enteromorpha prolifera based carbon for CO_2 capture. J Hazard Mater 2012;183(91):229–30.
[9] Li J-R, Ma Y, McCarthy MC, Sculley J, Yu J, Jeong H-K, et al. Carbon dioxide capture-related gas adsorption and separation in metal-organic frameworks. Coord Chem Rev 2011;255(15–16):1791–823.
[10] Sumida K, Rogow DL, Mason JA, McDonald TM, Bloch ED, Herm ZR, et al. Carbon dioxide capture in metal-organic frameworks. Chem Rev 2012;112(2):724–81.
[11] Furukawa H, Yaghi OM. Storage of hydrogen, methane, and carbon dioxide in highly porous covalent organic frameworks for clean energy applications. J Am Chem Soc 2009;131(25):8875–83.
[12] Feng X, Ding X, Jiang D. Covalent organic frameworks. Chem Soc Rev 2012;41(18):6010–22.
[13] Zhao YF, Yao KX, Teng BY, Zhang T, Han Y. A perfluorinated covalent triazine-based framework for highly selective and water-tolerant CO_2 capture. Energy Environ Sci 2013;6(12):3684–92.
[14] Saha D, Bao ZB, Jia F, Deng SG. Adsorption of CO_2, CH_4, N_2O, and N_2 on MOF-5, MOF-177, and zeolite 5 Å. Environ Sci Technol 2010;44(5):1820–6.
[15] Akhtar F, Liu QL, Hedin N, Bergström L. Strong and binder free structured zeolite sorbents with very high CO_2-over-N_2 selectivities and high capacities to adsorb CO_2 rapidly. Energy Environ Sci 2012;5(6):7664–73.
[16] Kim BJ, Cho KS, Park SJ. Copper oxide-decorated porous carbons for carbon dioxide adsorption behaviors. Colloid Interface Sci 2010;342(2):575–8.
[17] Bhagiyalakshmi M, Hemalatha P, Ganesh M, Mei PM, Jang HT. A direct synthesis of mesoporous carbon supported MgO sorbent for CO_2 capture. Fuel 2011;90(4):1662–7.
[18] Sevilla M, Fuertes AB. Sustainable porous carbons with a superior performance for CO_2 capture. Energy Environ Sci 2011;4(5):1765–71.
[19] Hao G, Li W, Qian D, Lu A. Rapid synthesis of nitrogen-doped porous carbon monolith for CO_2 capture. Adv Mater 2010;22(7):853–7.
[20] Wickramaratne NP, Jaroniec M. Importance of small micropores in CO_2 capture by phenolic resin-based activated carbon spheres. J Mater Chem A 2013;1(1):112–6.
[21] Jin Y, Hawkins SC, Huynh CP, Su S. Carbon nanotube modified carbon composite monoliths as superior sorbents for carbon dioxide capture. Energy Environ Sci 2013;6(9):2591–6.
[22] Wei H, Deng S, Hu B, Chen Z, Wang B, Huang J, et al. Granular bamboo-derived activated carbon for high CO_2 adsorption: the dominant role of narrow micropores. ChemSusChem 2012;5(12):2354–61.
[23] Sevilla M, Valle-Vigón P, Fuertes AB. N-doped polypyrrole based porous carbons for CO_2 capture. Adv Funct Mater 2011;21(14):2781–7.
[24] Presser V, McDonough J, Yeon S-H, Gogotsi Y. Effect of pore size on carbon dioxide sorption by carbide derived carbon. Energy Environ Sci 2011;4(8):3059–66.
[25] Yazaydin AO, Snurr RQ, Park T, Koh K, Liu J, LeVan MD, et al. Screening of metal-organic frameworks for carbon dioxide capture from flue gas using a combined experimental and modeling approach. J Am Chem Soc 2009;131(51):18198–9.

[26] Wickramaratne NP, Jaroniec M. Activated carbon spheres for CO_2 adsorption. ACS Appl Mater Interfaces 2013;5(5):1849–55.
[27] Dziure A, Marszewski M, Choma J, de Souza Luiz KC, Osuchowski L, Jaroniec M. Saran-derived carbon for CO_2 and benzene sorption at ambient conditions. Ind Eng Chem Res 2014;53(40):15383–8.
[28] Romanos J, Beckner M, Rash T, Firlej L, Kuchta B, Yu P, et al. Nanospace engineering of KOH activated carbon. Nanotechnology 2012;23(1):015401.
[29] de Souza LKC, Wickramaratne NP, Ello A, Costa MJF, da Costa CEF, Jaroniec M. Enhancement of CO_2 adsorption on phenolic resin-based mesoporous carbons by KOH activation. Carbon 2013;65:334–40.
[30] Kemp KC, Chandra V, Saleh M, Kim KS. Reversible CO_2 adsorption by an activated nitrogen doped graphene/polyaniline material. Nanotechnology 2013;24(23):235703.
[31] Adeniran B, Masika E, Mokaya R. A family of microporous carbons prepared via a simple metal salt carbonization route with high selectivity for exceptional gravimetric and volumetric post-combustion CO_2 capture. J Mater Chem A 2014;2(35):14696–710.
[32] Zhao Y, Liu X, Yao K-X, Zhao L, Han Y. Superior capture of CO2 achieved by introducing extra-framework cations into N-doped microporous carbon. Chem Mater 2012;24(24):4725–34.
[33] Zhao YF, Zhao L, Yao KX, Yang Y, Zhang Q, Han Y. Novel porous carbon materials with ultrahigh nitrogen contents for selective CO_2 capture. J Mater Chem 2012;22(37):19726–31.
[34] Ma X, Li Y, Cao M, Hu C. A novel activating strategy to achieve highly porous carbon monoliths for CO_2 capture. J Mater Chem A 2014;24(2):4819–26.
[35] Seredych M, Jagiello J, Bandosz TJ. Complexity of CO_2 adsorption on nanoporous sulfur-doped carbons – is surface chemistry an important factor? Carbon 2014;74. 207-7.
[36] Seema H, Kemp KC, Le NH, Park SW, Chandra V, Lee JW, et al. Highly selective CO_2 capture by S-doped microporous carbon materials. Carbon 2014;66:320–6.
[37] Zhou H, Xu S, Su H, Wang M, Qiao W, Ling L, et al. Facile preparation and ultra-microporous structure of melamine–resorcinol–formaldehyde polymeric microspheres. Chem Commun 2013;49(36):3763–5.
[38] Rouquerol J, Llewellyn P, Rouquerol F. Is the BET equation applicable to microporous adsorbents? Stud Surf Sc Catal 2007;160:49–56.
[39] Walton KS, Snurr RQ. Applicability of the BET method for determining surface areas of microporous metal-organic frameworks. J Am Chem Soc 2007;129(27):8552–6.
[40] Wang M, Wang JT, Qiao WM, Ling LC, Long DH. Scalable preparation of nitrogen-enriched carbon microspheres for efficient CO_2 capture. RSC Adv 2014;4(106):61456–64.
[41] Wickramaratne NP, Xu J, Wang M, Zhu L, Dai LM, Jaroniec M. Nitrogen enriched porous carbon spheres: attractive materials for supercapacitor electrodes and CO_2 adsorption. Chem Mater 2014;26(9):2820–8.
[42] Feng SS, Li W, Shi Q, Li YH, Chen JC, Ling Y, et al. Synthesis of nitrogen-doped hollow carbon nanospheres for CO_2 capture. Chem Commun 2014;50(3):329–31.
[43] Hu X, Radosz M, Cychosz KA, Thommes M. CO_2-filling capacity and selectivity of carbon nanopores: synthesis, texture, and pore-size distribution from quenched-solid density functional theory (QSDFT). Environ Sci Technol 2011;45(16):7068–74.
[44] Hummers WS, Offeman RE. Preparation of graphitic oxide. J Am Chem Soc 1958;80(6):1339.
[45] Myers AL, Prausnitz JM. Thermodynamics of mixed-gas adsorption. AIChE J 1965;11(1):121–7.
[46] Bae YS, Mulfort KL, Frost H, Ryan P, Punnathanam S, Broadbelt LJ, et al. Separation of $CO_{(2)}$ from $CH_{(4)}$ using mixed-ligand metal-organic frameworks. Langmuir 2008;24(16):8592–8.